ISSN (ONLINE): 2455-9261

SOUTH ASIAN JOURNAL OF RESEARCH IN ENGINEERING SCIENCE AND TECHNOLOGY (SAJREST)

VOLUME: 01 ISSUE: 05 WWW.SAJREST.COM

ANALYSIS OF ABSORPTION AND SCATTERING CROSS-SECTIONS OF Au/AlGaAs/GaAs CORE-MULTISHELL NANOWIRE

Sakin S. Satter[1], *Sabera Fahmida Shiba*[2], *Farhana Anwar*[3], *Rafee Mahbub*[4], *A.B.M. Hasan Talukder*[5]
University of Dhaka,
Department of Electrical and Electronic Engineering,
Nilkhet, Dhaka – 1000, Bangladesh.
sakin.sarwar1993@gmail.com

***Abstract* – Absorption and Scattering cross section of Au/AlGaAs/GaAs single core-multishell nanowire has been analyzed using the Finite-Difference Time-Domain (FDTD) simulation. The source used in the simulation is a Total-Field Scattered-Field (TFSF) which ranged from 300-900 *nm*. Strong scattering cross section is observed from the σ_{scat} versus wavelength (λ) curve. Increase in absorption cross section is also observed due to GaAs and AlGaAs having direct bandgaps. For core radii of 25 *nm*, 35 *nm* and 45 *nm* σ_{scat} increases respectively. The increase in thickness of AlGaAs layer elevated the scattering cross section far greater than the increase in thickness of the Au layer and the joint increase in thickness of the Au/AlGaAs layer increases the spectral linewidth. Shifts in wavelength (λ) is also observed as the radius of the core-multishell NW increases. Such high optical scattering properties can be used in infra-red lasing operations. Since there is a surface passivation of AlGaAs, the core multi-shell NW is also useful as photodetectors**

***Keywords* - core-multishell nanowire; scattering cross section; absorption cross section; III-V semiconductors; localized surface plasmon resonance**

ISSN (ONLINE): 2455-9261

SOUTH ASIAN JOURNAL OF RESEARCH IN ENGINEERING SCIENCE AND TECHNOLOGY (SAJREST)

VOLUME: 01 ISSUE: 05 WWW.SAJREST.COM

I. INTRODUCTION

Semiconductor nanowires (NWs) are the pre-eminent choice for optoelectronics, nanoelectronics and sensors. Adding a thin metal layer makes semiconductor NWs a pristine selection for further enhancing their role in the sub-field of photonics [1]. Gallium Arsenide (GaAs) shows superior electrical and optical properties for being a III-V semiconductor [2]. Core multi-shell NWs present the options of regulating the size of the core and the radial shell(s) respectively. GaAs/AlGaAs system has a very small lattice mismatch between them (about ~0.12%) and is thus an exemplary option to form strain-free axial and radial heterostructured NWs [3]. Application of single NWs can be nanolasers since they function as Fabry-Pérot (F-P) microcavity which provides good optical feedback for lasing [4-6]. The large density of surface states of the III-V NWs degrades the surface characteristics by pinning the surface Fermi energy. These surface states act as non-radiative carrier traps. The AlGaAs shell passivates the GaAs core diminishing these surface defects [7]. Metal shells having plasmonic properties introduces the phenomenon of Surface Plasmon Resonance and further enhancing the scattering characteristics.

In this work, Au/AlGaAs/GaAs core multi-shell NW has been designed by the help of FDTD modeling. The simulated NW is illuminated by TFSF source under a specific mesh settings. σ_{scat} and σ_{abs} is visualized in the simulation program and then compared for various radii of the core, also with changing the thickness of the shells.

II. DESIGN AND SIMULATION

The proposed NW structure is of a core-multishell type with the core being GaAs along with successive AlGaAs and Au shells respectively.

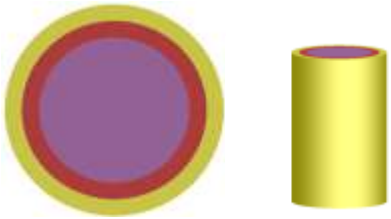

(a) (b)

Fig. 1. (a) XY view of the proposed Au/AlGaAs/GaAa core-multishell NW. (b) Perspective view of the core-multishell NW.

In Fig.1 the GaAs core (purple) is surrounded by the AlGaAs shell (brick red) and a final shell of Au (yellow). For this analysis we have used a core radii of 25 nm, 35 nm, and 45 nm. The thickness of the two consecutive shells were kept at 2 nm. The core-multishell nanowire was illuminated by a TFSF source having a wavelength range of 300 nm to 900 nm. The thickness of Au and AlGaAs was also changed and its effects were recorded.

The source selected is a TFSF source within the wavelength range of 300 nm-900 nm. The modeled source parameters are shown in Table I.

Table I. Modeled Source Parameters.

Tab	Property	Value
General	Polarization angle	0
	Injection Axis	y-axis
Geometry	x (nm)	0
	y (nm)	0
	x span (nm)	100
	y span (nm)	100
Frequency/Wavelength	Wavelength Start (nm)	300
	Wavelength Stop (nm)	900

The simulation parameters include the FDTD modeling and the mesh modeling which are included in the Table II. and Table III. respectively.

Table II. 2D FDTD Modeling Parameters.

Tab	Property	Value
General	Simulation time (fs)	200
	Dimension	2D
	Background Index	1
Geometry	x (nm)	0
	y (nm)	0
	z (nm)	0
	x span (nm)	800
	y span (nm)	800
Mesh Settings	Mesh accuracy	4
	Mesh refinement	Conformal variant 1
Boundary Conditions	x min bc	PML
	x max bc	PML
	y min bc	PML
	y max bc	PML

Table III. Mesh Modelling Parameters

Tab	Property	Value
General	Override x mesh [dx (nm)]	1
	Overide y	1

ISSN (ONLINE): 2455-9261

SOUTH ASIAN JOURNAL OF RESEARCH IN ENGINEERING SCIENCE AND TECHNOLOGY (SAJREST)

VOLUME: 01 ISSUE: 05 WWW.SAJREST.COM

	mesh [dy (nm)]	
Geometry	x (nm)	0
	y (nm)	0
	x span (nm)	110
	y span (nm)	110

The Time Monitor setup simulation parameters are given in Table IV. The Analysis Group involves the Total Analysis Group and the Scattering Analysis Group as shown in Table V. and Table VI. respectively.

Table IV. Time Monitor Setup Simulation Parameters.

Tab	**Property**	**Value**
	Name	time
General	Start Time (fs)	0
	Stop Time (fs)	200
	Simulation Type	All
Geometry	Monitor Type	Point
	x (nm)	28
	y (nm)	26
Advanced	min sampling per cycle	10
	Sampling rate (THz)	18223.5
	Down sample time	47

Table V. Total Analysis Group Simulation Parameters.

Tab	**Property**	**Value**
	Name	total
Setup -> Variables	x (nm)	0
	y (nm)	0
	x span (nm)	90
	y span (nm)	90

Table VI. Scattering Analysis Group Simulation Parameters.

Tab	**Property**	**Value**
	Name	scat
Setup -> Variables	x (nm)	0
	y (nm)	0
	x span (nm)	110
	y span (nm)	110
	z span (nm)	110*

III. RESULT AND ANALYSIS

Single GaAs and single core-multishell Au/AlGaAs/GaAs NWs have been compared. Both the studies have been done for GaAs core radii of 25 nm, 35 nm and 45 nm. In Fig. 2. we can see both the absorption and the scattering cross sections for GaAs NW and Au/AlGaAs/GaAs NW. From Fig. 2.(a and c), for a radius of 25 nm, the GaAs NW gets a peak at 426 nm wavelength and the Au/AlGaAs/GaAs NW gets it at 430 nm. But the magnitude of the absorption cross section does not vary widely due to the addition of the Au/AlGaAs layer, it only increases with the increase in radius. It can be stated that the absorption cross section had a temperate change between the GaAs NW and the Au/AlGaAs/GaAs NW. As the radius of the NW increases a red shift is observed.

Analyzing Fig. 2.(b-d) the scattering cross section change can be determined. At a radius of 45 nm, the increase in scattering cross-section due to the addition of Au/AlGaAs layer is 15.6% greater than normal GaAs NW. This happens at a wavelength of 515 nm. For a radius of 35 nm the increase in $\sigma scat$ is about 40.65% more at λ=465 nm. Eventhough the increase in $\sigma scat$ is higher for 35 nm, the magnitude of $\sigma scat$ for 45 nm Au/AlGaAs/GaAs core multi-shell NW is much higher. The core-multishell NW has a greater scattering cross section compared to the GaAs NW for all three radii.

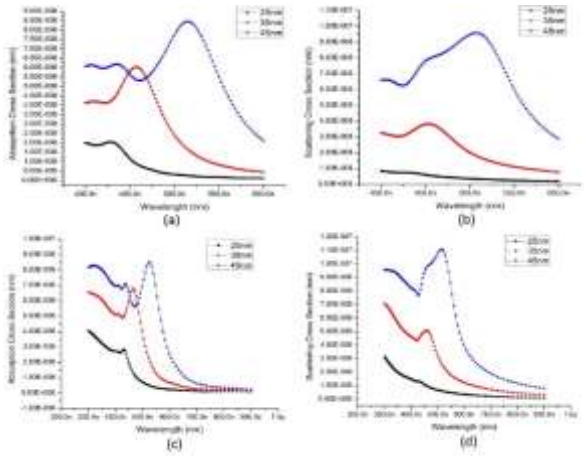

Fig. 2. (a-b) Absorption and Scattering cross sections respectively for GaAs NW. (c-d) Absorption and Scattering cross sections respectively for Au/AlGaAs/GaAs core-multishell NW.

ISSN (ONLINE): 2455-9261

SOUTH ASIAN JOURNAL OF RESEARCH IN ENGINEERING SCIENCE AND TECHNOLOGY (SAJREST)

VOLUME: 01 ISSUE: 05 WWW.SAJREST.COM

The introduction of the Au/AlGaAs layer has a great impact on scattering cross section of GaAs NW. We can further study the impact of the Au and AlGaAs layers both individually and merging the two layers as shown in Fig. 3.

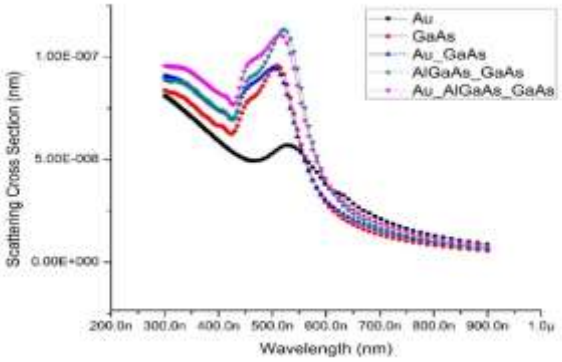

Fig. 3. Effect of different shells (Au and AlGaAs) on the GaAs NW.

The AlGaAs shell heavily increases the scattering cross section of the GaAs NW whereas the Au layer increases the spectral linewidth of the scattering cross section. The graph in Fig. 3. is for a core of radius 35nm and the layers have a thickness of 2nm. This core-shell heterostructure is possible because of the matching lattice constants of GaAs and AlGaAs [8]. Due to the abrupt termination of a semiconductor crystal (hindering the periodicity of the lattice structure at the surface), a large number of electrically active states are formed [9]. The abrupt termination in the periodicity of the lattice gives to surface dangling bonds which introduce electronic energy levels inside the normally forbidden semiconductor bandgap referred to as surface or interface states. Such states greatly enhance the non-radiative electron-hole recombination (Surface and Auger recombination) which decreases the scattering efficiency [10]. The AlGaAs layer passivates these dangling bonds reducing the non-radiative recombination [11].

Finally, the Au layer being a metal exhibits strong plasmonic characteristics. Localized Surface Plasmon Resonance (LSPR) is observed since we are considering dimensions in the nano level. In Fig. 2.(d) we can see that as the radius increases for the Au/AlGaAs/GaAs core-multishell NW, the peak of the scattering cross section shifts to the right. This strong surface plasmon peak in the far red region originates from the phase retardation effect [12]. The spectral linewidth is controlled by the phase retardation effect. The phase retardation is also accountable for the excitation of sharp higher order of plasmon modes [13].

The effect of thickness on the scattering cross section have also been observed as in Fig. 4. The thicknesses of both Au and AlGaAs layer has been set to 4 *nm*, 6 *nm*, and 8 *nm*. Keeping the thickness of AlGaAs constant (2 *nm*), the increase in Au thickness elevated the scattering cross section. Conversely, increasing the AlGaAs layer thickness gave a higher scattering cross section than the increase of Au layer thickness. A combined increase in thickness, resulted in a higher scattering cross section as well as a wider spectral linewidth.

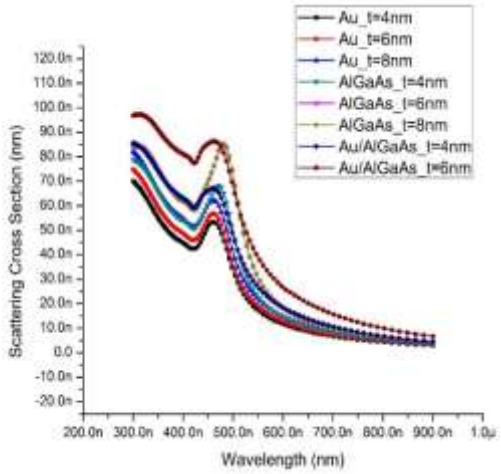

Fig. 4. Effect of thickness change on Au/AlGaAs/GaAs core-multishell NW.

IV. CONCLUSION

We have performed FDTD mathematical modeling to reveal the optical properties namely scattering and absorption cross-sections of Au/AlGaAs/GaAs core multi-shell NW. The GaAs NW has a zinc blende structure which is typically included in the Lumerical FDTD Solutions database. The results from the simulation revealed riveting facts about the optical scattering of the NW. Increase in the radius increases the scattering cross-section drastically and comparing with GaAs NW, the increase in $\sigma scat$ for Au/AlGaAs/GaAs is almost 15.6%. We can also observe a wavelength shift which can be established as a result of the surface plasmon resonance of the metal coating of the NW. In our designed FDTD model, the background has been considered as air medium.

Thus there is a metal-air dielectric interface, since the outermost layer of the core-multishell NW is of Au. Since scattering is the principal characteristic for study these types of NWs are commonly used for lasing applications. Single-mode continuous wave (CW) lasing can be obtained from individual Au/AlGaAs/GaAs NW subject to optical excitation. Due to the broadening of the spectral linewidth, this NW can used for wide range photodetectors, with low selectivity. These can be used in Active-Pixel sensors. For an AlGaAs thickness of t = 6 nm and t = 8 nm keeping Au thickness constant (2 nm), the selectivity is high and can be used for specific wavelength photodetectors such as quantum-well infra-red photodetectors [14].

REFERENCES

[1] MJ Tambe1, LF Allard and S Gradečak, "Characterization of core-shell GaAs/AlGaAs nanowire heterostructures using advanced electron microscopy", *Journal of Physics*: Conference Series 209 (2010) 012033

[2] Haomin Guo, Long Wen, Xinhua Li, Zhifei Zhao and Yuqi Wang, "Analysis of optical absorption in GaAs nanowire arrays", Guo et al. *Nanoscale Research Letters* 2011, 6:617

[3] H. L. Zhou, T. B. Hoang, D. L. Dheeraj, A. T. J. van Helvoort, L. Liu, J. C. Harmand, B. O. Fimland and H. Weman, "Wurtzite GaAs/AlGaAs core–shell nanowires grown by molecular beam epitaxy", *Nanotechnology* 20 (2009) 415701 (7pp)

[4] X. Duan, Y. Huang, R .Agarwal and C. M. Lieber, "Single-nanowire electrically driven lasers", *Nature*, 2003, 421, 241

[5] B. Hua, J. Motohisa, Y. Ding, S. Hara and T. Fukui, "Characterization of Fabry-Pérot microcavity modes in GaAs nanowires fabricated by selective-area metal organic vapor phase epitaxy", *Appl. Phys. Lett*., 2007, 91, 131112

[6] Y. Ding, J. Motohisa, B. Hua, S. Hara and T. Fukui, "Observation of Microcavity Modes and Waveguides in InP Nanowires Fabricated by Selective-Area Metalorganic Vapor-Phase Epitaxy", *Nano Lett*., 2007, 7, 3598-3602

[7] Xing Dai, Sen Zhang, Zilong Wang, Giorgio Adamo, Hai Liu, Yizhong Huang, Christophe Couteau, and Cesare Soci1, "GaAs/AlGaAs Nanowire Photodetector", *Nano Lett*., 2014, 14 (5), pp 2688–2693

[8] Hannah J. Joyce, Y. Kim, Q. Gao, H. H. Tan, C. Jagadish, Growth, "Structural and Optical Properties of GaAs/AlGaAs Core/Shell Nanowires with and without Quantum Well Shells", 2006 International Conference on Nanoscience and *Nanotechnology*, Brisbane, Qld., 2006, pp.

[9] eee.colorado.edu/~bart/book/book/chapter2/ch2_8.htm

[10] Black, Lachlan E, "New Perspectives on Surface Passivation: Understanding the Si-Al2O3 Interface", Chp-2, Surface Recombination Theory, Pg: 15-28, ISBN 978-3-319-32521-7

[11] Benedikt Mayer, Daniel Rudolph, Joscha Schnell, Stefanie Morkotter, Julia Winnerl, Julian Treu, Kai Muller, Gregor Bracher, Gerhard Abstreiter, Gregor Koblmuller and Jonathan J. Finley, "Lasing from individual GaAs-AlGaAs core-shell nanowires up to room temperature", *Nature Communications* 4, Article number: 2931

[12] Sang-Youp Yim, Hong-Gyu Ahn, Koo-Chul Je, Moohyun Choi, Chang Woo Park, Honglyoul Ju, and Seung-Han Park, "Observation of red-shifted strong surface plasmon scattering in single Cu nanowires", 6 August 2007 / Vol. 15, No. 16/ *Optics Express* 10287

[13] S. L. Westcott, J. B. Jackson, C. Radloff, and N. J. Halas, "Relative contributions to the plasmon line shape of metal nanoshells", *Physical Review B* 66, 155431 (2002)

[14] B. F. Levine, "Quantum-well infrared photodetectors", *J. Appl. Phys*. 74, R1 (1993)